# Final-state screening dynamics in resonant Auger decay at the 2*p* edge of vanadium

V. Ilakovac,[1,2,*] M. Kralj,[3] P. Pervan,[3] M. C. Richter,[1] A. Goldoni,[4] R. Larciprete,[4] L. Petaccia,[4] and K. Hricovini[1]
[1]*Laboratoire de Physique des Matériaux et des Surfaces, Université de Cergy-Pontoise, Neuville sur Oise, 95031 Cergy-Pontoise Cedex, France*
[2]*Laboratoire de Chimie Physique, Matière et Rayonnement (UMR 7614), Université P. et M. Curie, 11, rue P. et M. Curie, 75231 Paris, France*
[3]*Institute of Physics, P. O. Box 304, 10000 Zagreb, Croatia*
[4]*Elettra Synchrotron Light Source, S. S. 14-Km. 163.5, 34012 Basovizza, Trieste, Italy*
(Received 19 February 2004; revised manuscript received 11 October 2004; published 15 February 2005)

We investigated the resonant Auger process near the V $2p_{3/2}$ edge in vanadium metal. Attention is centered on the onset of Auger decays and their behavior below the $2p_{3/2}$ resonance. The $2p_{3/2}3d3d$ decay has a crossover from the Raman-Auger to the normal Auger regime at the 2*p* ionization threshold. Meanwhile, Auger decays with core holes in the final state have normal Auger behavior even below the ionization threshold, the $2p_{3/2}3p3p$ process being visible at 2.2 eV lower photon energy. The different resonant behavior of these Auger decays can be understood within the one-step model as final-state screening effects affecting the photoexcitation.

DOI: 10.1103/PhysRevB.71.085413 PACS number(s): 79.60.Bm, 33.60.Fy, 71.20.Be, 78.70.Dm

## I. INTRODUCTION

Resonant photoemission of the valence band is a powerful way to extend the information that can be obtained on the electronic structure of matter beyond the level given by standard photoemission experiments. In resonant photoemission the incoming photons have an energy which is in the vicinity of a core level absorption threshold, giving chemical element specificity in the analysis of the valence band spectrum. Since this method permitted clarification of the origin of the Ni two-hole satellite,[1] many studies have been performed both at the 3*p* edge[2–7] and at the 2*p* edge of 3*d* transition metals.[8–13] Resonant valence band studies at the 3*p* edge revealed the existence of subthreshold Auger processes.[1–7] They were confirmed by further studies at the 2*p* edge.[8–13] In contrast to the normal Auger electron behavior *above* threshold, whose energy is independent of the photon excitation, the energy of the emitted electron *below* the absorption threshold follows the photon energy. This constant "binding energy" behavior as a function of the photon energy is the so-called nonradiative Raman-Auger effect. It is the signature of an interaction between the photoexcited and the autoionized electrons.

For $2p3d3d$ Auger decay, which is superimposed on the valence band photoemission, the Raman-Auger to normal Auger crossover is well studied for some transition metals. The crossover is defined as the intersection of the lines defining the linear kinetic vs photon energy dependence of the Raman-Auger regime and the constant kinetic energy of the normal Auger behavior. With some exceptions, it is related to the ionization threshold (IT), measured as the binding energy (BE) of the 2*p* level, which is the smallest energy needed to excite an electron from the core level to the valence band. In nickel, the crossover is observed at the absorption maximum (resonance energy),[9] which coincides with the photon energy corresponding to the IT.[12] The resonance energy in iron and chromium is shifted to 0.9 and 2.0 eV higher energy relative to the IT, respectively. The crossover is observed at $\approx$2 eV below the 2*p* absorption maximum for both metals, i.e., at the IT for Cr and 1.1 eV below the IT for Fe.[12] For titanium, the resonance energy is shifted to 3 eV higher photon energy compared to the Ti 2*p* IT.[10] Raman-Auger behavior was not reported, but the onset of the $2p3d3d$ normal Auger decay is observed at the photon energy corresponding to the IT.

For 3*d* transition metals, the Raman-Auger to normal Auger crossover of Auger decays with final-state core holes is more rarely studied than that of the $2p3d3d$ decay. In nickel metal, the $2p3p3p$ Auger spectrum has been shown to have the same behavior as the $2p3d3d$ spectrum, i.e., resonant Raman-Auger below the photoabsorption maximum and normal Auger above.[11] For manganese, the $2p3p3p$ and $2p3p3d$ Auger decays have been reported to have a normal Auger behavior below resonance.[13]

Vanadium is an early 3*d* transition metal interesting for its magnetic properties when diluted in alloys.[14] As it is very reactive, studies of electronic properties of clean vanadium are quite rare. It is well studied by ultraviolet[15,16] and x-ray[17] photoemission spectroscopy. A resonant photoemission study was reported for the soft x-ray range.[5] Resonant studies at higher photon energies are necessary to improve the knowledge of its electronic structure, to complete the valence band studies of 3*d* transition metals, and to understand the 2*p* excitation dynamics not affected by strong electron correlations.

We report here the study of vanadium Auger decays at the $2p_{3/2}$ threshold. Auger spectra with different final states are measured simultaneously in order to have insight into any possible differences in their subthreshold behavior. The $2p3d3d$ Auger decay is found to have a normal Auger onset at the IT, as reported for titanium, chromium, and iron.[10,12] For photon energies lower than the IT, the Raman-Auger decay is observed at 2.3 eV BE relative to the Fermi level ($E_F$). It can be related to the two-hole correlation satellite, attainable only by the Auger channel, as in the case of chromium and iron.[12] Meanwhile, for Auger processes with core

 

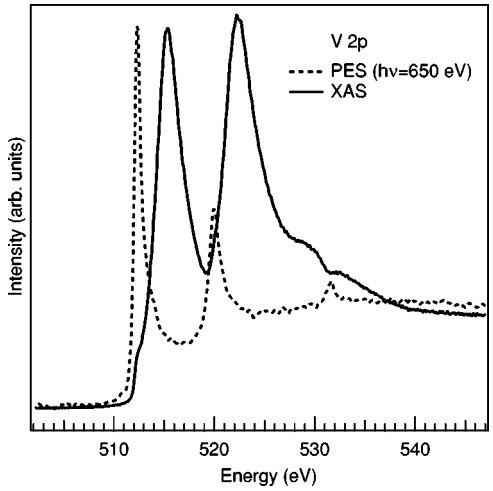


FIG. 1. V 2*p* PES spectrum at $h\upsilon = 650$ eV (dashed) and XAS spectrum (solid). The energy is the BE for the photoemission and the photon energy for the absorption. The dip on the high-energy side of the XAS spectrum is due to oxygen contamination of the beamline.

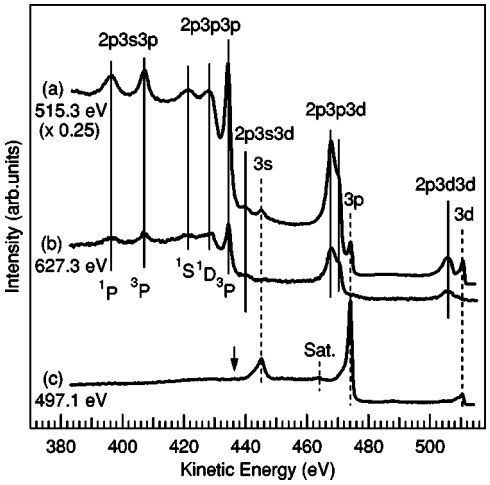


FIG. 2. V 2*p* Auger spectra (a) at the V $2p_{3/2}$ resonance energy, (b) at 112 eV above, and (c) at 18.2 eV below the resonance. Spectrum (c) is shifted by 18.2 eV to align the direct photoemission lines obtained at resonance. The absence of the Cu 3*p* signal at the position indicated by an arrow means that the Cu substrate is completely covered with vanadium.

holes in the final state, the normal Auger behavior is observed even *below* the IT. In addition, the process with two core holes in the final state is observed at lower photon energy than that with one final core hole. This relation between the number of final core holes and the onset of the normal Auger regime can be understood as a final-state screening effect.

The paper is organized as follows. First, we present the V 2*p* absorption and photoemission measurements which allow an accurate determination of the resonance energy and the IT. Further, the photon energy dependence of the 2*p*3*d*3*d* Auger decay is presented and discussed. Finally, the photon energy dependence of the 2*p*3*p*3*p* and 2*p*3*p*3*d* decays is given and discussed in terms of the core-hole screening in the final state.

## II. EXPERIMENT

The experiments were performed at the SuperESCA beamline of the Elettra storage ring, using a stigmatic SX-700 monochromator. The end station consists of a standard ultrahigh vacuum chamber equipped with a double-pass hemispherical electron analyzer with a 96-channel detector. The x-ray absorption spectra (XAS) were measured by collecting low-energy secondary electrons. The photon energy resolution of 160 meV (at 650 eV) and the analyzer resolution of 100–120 meV are comparable to the V $2p_{3/2}$ lifetime broadening of 180 meV.[18] The correct positions of electron spectra structures are determined by adjusting the BE of the Fermi level.

A thick layer of vanadium was deposited by an electron-bombardment evaporator. The Cu(100) substrate was cleaned by repeated cycles of argon ion sputtering and annealing at 450 °C. Evaporation permitted us to have a clean vanadium surface in a much shorter time than by cleaning a single crystal. The base pressure was $8 \times 10^{-11}$ mbar and the pressure during evaporation was about $10^{-10}$ mbar. Photoelectron spectra were used as a test for the cleanliness of the sample and the absence of any Cu contribution to the spectra.

## III. RESULTS AND DISCUSSION

### A. Determination of the resonance energy and the ionization threshold

The V 2*p* photoelectron spectrum (PES) induced by 650 eV photons and the V 2*p* XAS spectrum are shown on the same energy scale in Fig. 1. The positions of the V $2p_{3/2}$ and V $2p_{1/2}$ PES maxima relative to the $E_F$ are measured to be at 512.3 and 520.0 eV, respectively. We refer these energies to the V $2p_{3/2}$ and V $2p_{1/2}$ IT's. A small O 1*s* signal visible at a BE of 531.7 eV is due to oxygen contamination of the vanadium surface. The quantity of oxygen is estimated to be about 11% from the V 2*p* to O 1*s* ratio weighted by the corresponding photoabsorption cross sections.[19] The V 2*p* XAS corresponds to the $2p^6 3d^n \rightarrow 2p^5 3d^{n+1}$ transitions. The V $2p_{3/2}$ and V $2p_{1/2}$ absorption maxima (resonant energies) are located at 515.3 and 522.4 eV, respectively. It should be noted that the V $2p_{3/2}$ absorption maximum is shifted by 3 eV to higher energy with respect to the V $2p_{3/2}$ IT. The energy separation between the main components of the XAS spectrum is 0.6 eV smaller than the one in the PES spectrum. The transfer of the spectral weight away from the threshold and the apparent reduction in the spin-orbit splitting are attributed to the strong Coulomb and exchange interactions between the 2*p* core hole and the 3*d* electrons in the final state.[20]

### B. V 2*p* resonant Auger decays

Figure 2 shows the electron energy spectra recorded at the photon energy of the *V* $2p_{3/2}$ resonance ($h\nu = 515.3$ eV) (a), 112 eV above (b), and 18.25 eV below (c) the resonance

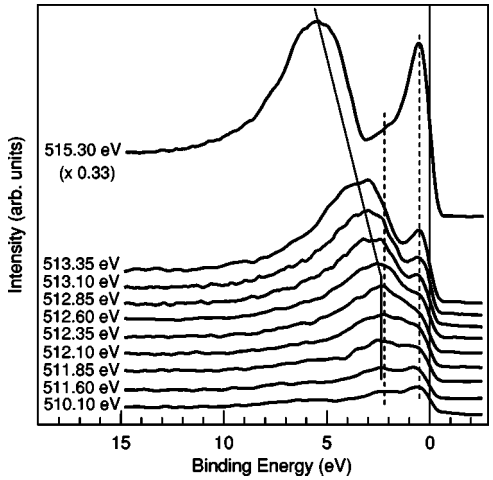


FIG. 3. Resonant behavior of the spectra in the valence band BE region, from the photon energy of 510.1 eV up to the resonance.

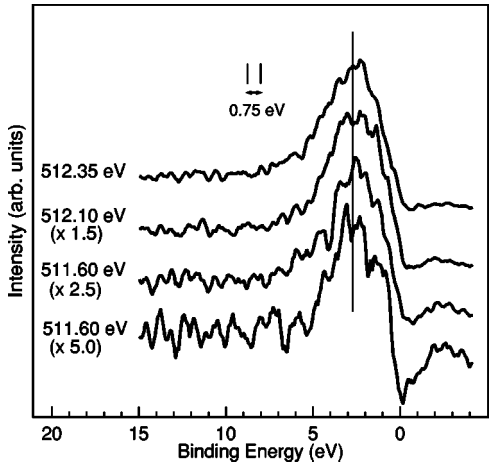


FIG. 4. Photon energy dependence of the V $2p_{3/2}3d3d$ nonradiative decay, from 3.7 to 3.0 eV below the V $2p_{3/2}$ resonance. The V $3d$ PES spectrum at 510.1 eV is subtracted from all the spectra. The spectra are normalized to the same height (the normalization factor is indicated in the figure).

energy. The spectrum far below resonance (c) is shifted to 18.2 eV higher kinetic energy to match the photoemission lines at resonance. Solid lines indicate Auger structures and dashed lines direct PES positions ($3s$, $3p$, $3d$, and "Sat." for $3p$ satellite). The arrow indicates the position where the Cu $3p$ line should be observed if the V layer was not sufficently thick to cover the copper substrate completely. On the left side of the figure, one observes the $2p_{3/2}3s3p$ Auger decay (the $3/2$ subscript is omitted in the figure for brevity). The $3s$-$3p$ Coulomb interaction in the final state is responsible for the $^1P$ and $^3P$ signals separated by 10.8 eV. The $2p_{3/2}3p3p$ Auger decay appears in the 420–437 eV kinetic energy (KE) range. It consists of the three ($^1S$, $^1D$, and $^3P$) $LS$ components arising from the Coulomb interaction between the two $3p$ holes in the final state. The intensity of the $^3P$ component at resonance is increased by a factor of 12 with respect to its value far above the resonance. The $2p_{3/2}3p3d$ Auger decay (460–475 eV) has at least two major contributions. According to the calculations performed on nickel[22] and iron,[23] we identified the low-energy component as a mixed ($^1P$, $^1F$) final state and the high-energy component as a mixed ($^3P$, $^3D$) final state. This line is superimposed on the $3p$ spectrum below the resonance. Finally, the $2p_{3/2}3d3d$ Auger decay is located in the right part of the figure (500–510 eV) and is superimposed on the valence band photoemission for photon energies close to the resonance.

#### *1. $2p_{3/2}3d3d$ Auger decay*

The resonant valence band behavior is shown in Fig. 3 for photon energies from 510.1 eV up to the resonance. The spectra are presented on the BE scale to show the expected Raman-Auger regime below the IT. Two structures at BE of 0.5 and 2.2 eV (dashed lines) do not change their position. They can be associated with the density of states contribution to the direct photoemission process.[21] The photon energy dependence of the $2p_{3/2}3d3d$ Auger process is indicated by a full line. For photon energies higher than 512.3 eV (IT), the $2p_{3/2}3d3d$ spectrum shifts with photon energy, so it has a normal Auger behavior. To bring to light the subthreshold $2p_{3/2}3d3d$ behavior, the V $3d$ PES's at 510.1 eV are subtracted from the valence band spectra. The subtracted spectra are shown in Fig. 4. The absence of the shift of the structure centered at a BE of 2.7 eV for different photon excitation signifies that the $2p_{3/2}3d3d$ decay has a Raman-Auger behavior below the IT. In the opposite case, the spectra recorded at 512.35 eV would be shifted to 0.75 eV higher binding energy relative to the spectra recorded at 511.60 eV. The Raman-Auger behavior of the $2p_{3/2}3d3d$ process can be related to the two-hole correlation satellite, attainable only through the Auger channel, as in the case of Cr and Fe.[12]

Our results are compared to studies on other $3d$ metals in Table I. The Raman-Auger position relative to the Fermi level increases from V to Ni, i.e., with electron correlations. At the same time, the difference between the photon energy of the Raman-Auger onset and the IT decreases drastically from Cr to V, and the Raman-Auger regime was not ob-

TABLE I. Comparing the $2p3d3d$ Auger decays of $3d$ transition metals: the Raman-Auger position relative to $E_F$, Raman-Auger onset, Raman to normal Auger crossover, and normal Auger onset relative to the IT. All values are in eV.

| | Raman-Auger position relative to $E_F$ | Raman-Auger onset | Raman to normal Auger crossover relative to the IT | Normal Auger onset |
|---|---|---|---|---|
| Ti[a] | | | | 0 |
| V[b] | 2.3 | 0.7 | 0 | 0 |
| Cr[c] | 3.5 | ≈5 | 0 | 0 |
| Fe[c] | 3.2 | ≈4 | ≈−1 | 0 |
| Ni[d] | 6.0 | ≈4 | 0 | ≈−0.5 |

[a]Reference 10.
[b]This work.
[c]Reference 12.
[d]Reference 9.

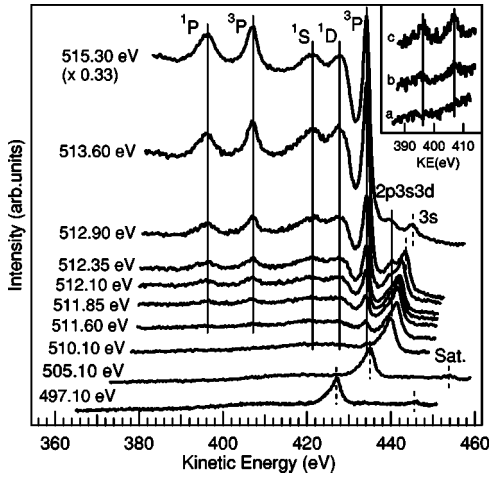


FIG. 5. Photon energy dependence of the V $2p_{3/2}3s3p$, $2p_{3/2}3p3p$ and $2p_{3/2}3s3d$ Auger spectra, from 18.2 eV below the V $2p_{3/2}$ resonance up to the resonance. "Sat." indicates the V $3p$ satellite. Inset shows the $2p_{3/2}3s3p$ KE region for photon energies (a) 510.10, (b) 511.60, and (c) 511.85 eV.

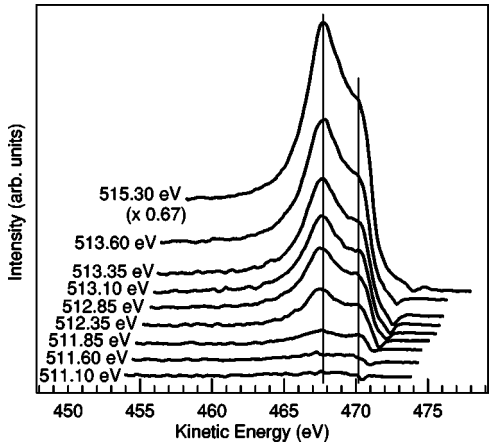


FIG. 6. Photon energy dependence of the V $2p_{3/2}3p3d$ Auger spectrum, from 4.2 eV below the V $2p_{3/2}$ resonance up to the resonance. The V $3p$ PES spectrum has been subtracted from all the spectra. The dip at 470-473 eV is an artifact of the subtraction and has no physical meaning.

served in Ti. The last two columns illustrate the influence of electron correlations on the transition from the Raman-Auger to the normal Auger behavior, i.e., from a single quantum-mechanical event to a process which can be separated into two steps. For light elements, like V and Cr, the two regimes join at the IT. Meanwhile, Fe has a mixed Raman–normal Auger behavior in an intermediate region of about 1 eV, while Ni switches rapidly from Raman to normal behavior at a photon energy about ≈0.5 eV below the IT.

#### *2. Auger decays with core holes in the final state*

The dependence of decays with two core holes in the final state on the excitation energy below resonance is shown in Fig. 5 on a KE scale. The most intense structure ($^3P$) of the $2p_{3/2}3p3p$ spectrum is visible when the photon energy is tuned to 510.1 eV (2.2 eV below the $2p_{3/2}$ IT). Its intensity does not change significantly up to an excitation energy of 511.6 eV. At this energy, a swelling of the background is observed, in the region where the two singlet structures grow up. The two $^1P$ and $^3P$ components of the $2p_{3/2}3s3p$ spectrum appear at 511.6 eV (see the inset of Fig. 5). The low-intensity $2p_{3/2}3s3d$ feature appears at the same photon energy as a shoulder on the low KE side of the V $3s$ PES peak (440 eV). Even below the IT, these nonradiative decays have a KE that does not change with photon energy: they have a normal Auger behavior.

The evolution of the $2p_{3/2}3p3d$ nonradiative decay with the photon energy, from 511.1 eV below the resonance up to the resonance, is given in Fig. 6 on a KE scale. The V $3p$ PES spectrum has been subtracted from the spectra. One can note that the $2p_{3/2}3p3d$ Auger structure appears at 511.6 eV, like the $2p_{3/2}3s3p$ and $2p_{3/2}3s3d$ spectra. Its position does not change with photon energy; thus this decay has also a normal Auger behavior, even below the IT.

Table II compares the Auger resonant behavior of three Auger decays with different final states. The differences in behavior of these Auger processes can be understood in terms of the final-state screening. It is known that in some cases, for instance in nickel metal, the main photoemission lines are accompanied by two-hole satellites. A schematic representation of the Kotani-Toyozawa model (see Refs. 24 and 25) explains this effect. This model predicts that after the photoionization of a core electron, the $d$ band is pulled down and its unoccupied states below $E_F$ produce an extra hole. We suggest that in a resonant decay, which has to be viewed below the IT as a one-step process, this $3d$ hole can accommodate not only a $4sp$ screening electron, but also the photoexcited $2p$ electron, thus permitting an absorption process below the IT.

We illustrate this in the case of the $2p_{3/2}3p3p$ decay. In the ground-state configuration, the $3d$ band is located at $E_F$ [Fig. 7(a)]. In the final state ($3p^4 3d^{n+1}$), the two $3p$ core holes are screened by a pulldown of the $3d$ band. The first screening process is shown in Fig. 7(b): the $3d$ band is pulled down and the unoccupied $3d$ states under $E_F$ accommodate the photoexcited electron. The screening is accomplished by $4sp$ electrons and the photoexcited electron in the $3d$ band. In the second screening process [Fig. 7(c)], the unoccupied levels in the pulled-down $3d$ band are filled by $4sp$ electrons. In this final state the photoexcited electron is accommodated at $E_F$. Note that in the first screening process, the photon energy needed for absorption is smaller, which permits the normal Auger line to appear below the IT.

TABLE II. Raman-Auger and normal Auger onset relative to the IT, for three V Auger decays with different final states.

| | Number of final-state core holes | Raman-Auger onset | Normal Auger onset |
|---|---|---|---|
| $2p_{3/2}3d3d$ | 0 | 0.7 eV | 0.0 eV |
| $2p_{3/2}3p3d$ | 1 | | 0.7 eV |
| $2p_{3/2}3p3p$ | 2 | | 2.2 eV |

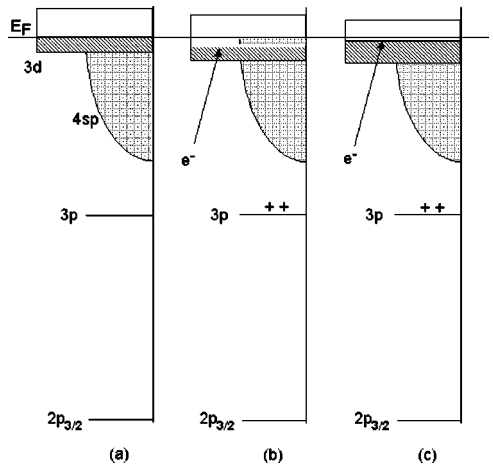


FIG. 7. Schematic representation of the model for screening in the $3p^4 3d^{n+1}$ final-sate configuration. (a) In the initial state, the metal $3d$ band is separated by $E_F$ into an occupied part and an unoccupied part. In the final state, (b) the $3d$ band is pulled down below $E_F$, and there are $3d$ holes below $E_F$ which accommodate the photoexcited electron, (c) $4sp$ electrons fill $3d$ hole states below $E_F$ and the photoexcited electron is accommodated at $E_F$.

In the $2p_{3/2}3p3p$ Auger processes the final state has two $3p$ holes and the $3d$ band has to be pulled down a lot to achieve their screening. The first screening channel permits photoexcited electrons to be accommodated below $E_F$. In the $2p_{3/2}3p3d$ process, there is only one $3p$ hole in the final state: the pulldown of the $3d$ band is smaller and the unoccupied $3d$ states are closer to $E_F$: the normal Auger behavior starts at a higher photon energy than the one of the $2p_{3/2}3p3p$ Auger process, but still below the IT. Contrary to decays with final-state core holes, the $2p_{3/2}3d3d$ process involves no final-state core hole and there is no need for pulling down the $3d$ band. To achieve photoabsorption below the IT, the photoexcited and autoionized electrons interact. The KE of the autoionized electron has a photon energy dependence and the Auger line has a Raman-Auger behavior. Above the IT, the photoexcited electron can be accommodated at $E_F$, and the Auger process has a normal Auger behavior.

It should be noted that the $2p_{3/2}3s3p$ decay does not appear at the same photon energy as the $2p_{3/2}3p3p$ decay, even if both have two core holes in the final state. In the last case, both electrons involved in the final state belong to the same shell. The probability of the $2p_{3/2}3p3p$ process is higher and permits it to be observed at a lower photon energy.

The effect of the different behavior of $2p3p3p$, $2p3p3d$, and $2p3d3d$ Auger decays is not observed in nickel metal[11] because the final state of the $2p_{3/2}3p3p$ Auger processes is $3p^4 3d^{10}$: the $3d$ band is occupied and the first screening channel is equivalent to the second one.

## IV. CONCLUSION

We report a resonant Auger study near the V $2p_{3/2}$ edge in vanadium metal. The study is centered on the very beginning of the absorption process and the behavior of the Auger decay lines below the resonance. The $2p_{3/2}3d3d$ decay has a constant binding energy up to the ionization threshold and a constant kinetic energy above. The Raman-Auger regime below threshold gives rise to the same final state as the two-hole correlation satellite, here attainable only through Auger channel, as in Cr and Fe.

The most intense $2p_{3/2}3p3p$ nonradiative decay is observed 2.2 eV below the ionization threshold. Its constant kinetic energy position shows that it is a normal Auger process. The $2p_{3/2}3d3d$ decay appears 0.7 eV below the ionization threshold and it has a normal Auger behavior too. This premature normal Auger behavior is understood in terms of screening of the core holes in the final state. As Auger decay is a single quantum-mechanical event below the ionization threshold, screening effects can affect the photoexcitation.

We show that the transition from the Raman-Auger to the normal Auger behavior of $3d$ transition metals should be discussed as an interplay between $3d$ electron correlations and final-state screening dynamics.

## ACKNOWLEDGMENTS

This work was supported by the Human Potential Programme, Transnational Access to Major Research Infrastructures, of the European Community and by the Ministry of Science and Technology of the Republic of Croatia (Project No. 0035016).

*Electronic address: ilakovac@ccr.jussieu.fr

[1] C. Guillot, Y. Ballu, J. Paigné, J. Lecante, K. P. Jain, P. Thiry, R. Pinchaux, Y. Pétroff, and L. M. Falicov, Phys. Rev. Lett. **39**, 1632 (1977).

[2] D. Chandesris, J. Lecante, and Y. Petroff, Phys. Rev. B **27**, 2630 (1983).

[3] T. Kaurila, L. Säisä, and J. Väyrynen, J. Phys.: Condens. Matter **6**, 5053 (1994).

[4] T. Kaurila and J. Väyrynen, J. Electron Spectrosc. Relat. Phenom. **82**, 165 (1996).

[5] T. Kaurila, J. Väyrynen, and M. Isokallio, J. Phys.: Condens. Matter **9**, 6533 (1997).

[6] A. Gutiérrez and M. F. Lopez, Phys. Rev. B **56**, 1111 (1997).

[7] P. Pervan, M. Milun, and D. P. Woodruff, Phys. Rev. Lett. **81**, 4995 (1998); Fiz. A **8**, 35 (1999).

[8] L. H. Tjeng, C. T. Chen, J. Ghijsen, P. Rudolf, and F. Sette, Phys. Rev. Lett. **67**, 501 (1991).

[9] M. Weinelt, A. Nilsson, M. Magnuson, T. Wiell, N. Wassdahl, O. Karis, A. Föhlisch, N. Mårtensson, J. Stöhr, and M. Samant, Phys. Rev. Lett. **78**, 967 (1997).

[10] T. Kaurila, R. Uhrberg, and J. Väyrynen, J. Electron Spectrosc. Relat. Phenom. **88-91**, 399 (1998).

[11] M. Finazzi, G. Ghiringhelli, O. Tjernberg, and N. B. Brookes, J. Phys.: Condens. Matter **12**, 2123 (2000).

[12] S. Hüfner, S.-H. Yang, B. S. Mun, C. S. Fadley, J. Schäfer, E. Rotenberg, and S. D. Kevan, Phys. Rev. B **61**, 12 582 (2000).
[13] M. C. Richter, P. Bencok, R. Brochier, V. Ilakovac, O. Heckmann, G. Paolucci, A. Goldoni, R. Larciprete, J.-J. Gallet, F. Chevrier, G. van der Laan, and K. Hricovini, Phys. Rev. B **63**, 205416 (2001).
[14] M. Finazzi, E. Kolb, J. Prieur, Ch. Boeglin, K. Hricovini, G. Krill, C. Chappert, and J.-P. Renard, J. Magn. Magn. Mater. **165**, 373 (1997).
[15] P. Pervan, T. Valla, and M. Milun, Solid State Commun. **89**, 917 (1994).
[16] P. Pervan, T. Valla, M. Milun, A. B. Hayden, and D. P. Woodruff, J. Phys.: Condens. Matter **8**, 4195 (1996).
[17] P. Pervan, T. Valla, and M. Milun, Solid State Commun. **99**, 393 (1996).
[18] R. Nyholm, N. Mårtensson, A. Lebugle, and U. Axelsson, J. Phys. F: Met. Phys. **11**, 1727 (1981).
[19] J. J. Yeh and I. Lindau, At. Data Nucl. Data Tables **32**, 1 (1985).
[20] J. Zaanen, G. A. Sawatzky, J. Fink, W. Speier, and J. C. Fuggle, Phys. Rev. B **32**, 4905 (1985).
[21] B. Peric, T. Valla, M. Milun, and P. Pervan, Vacuum **46**, 1181 (1995).
[22] G. van der Laan, M. Surman, M. A. Hoyland, C. F. J. Flipse, B. T. Thole, Y. Seino, H. Ogasawara, and A. Kotani, Phys. Rev. B **46**, 9336 (1992).
[23] Yu. Kucherenko, B. Sinković, E. Shekel, P. Rennert, and S. Hulbert, Phys. Rev. B **62**, 5733 (2000).
[24] S. Hüfner, *Photoelectron Spectroscopy* (Springer-Verlag, Berlin, 1996), p. 74.
[25] A. Kotani, and Y. Toyozawa, J. Phys. Soc. Jpn. **37**, 912 (1974).